Geometry, kinematics, and acoustics of Tamil liquid consonants

Shrikanth Narayanan
AT&T Labs—Research, 180 Park Avenue, Florham Park, New Jersey 07932-0971

Dani Byrd
Haskins Laboratories, 270 Crown Street, New Haven, Connecticut 06511

Abigail Kaun
Department of Linguistics, Yale University, New Haven, Connecticut 06520

(Received 10 December 1997; revised 15 February 1999; accepted 15 May 1999)

Tamil is unusual among the world's languages in that some of its dialects have five contrasting liquids. This paper focuses on the characterization of these sounds in terms of articulatory geometry and kinematics, as well as their articulatory-acoustic relations. This study illustrates the use of multiple techniques—static palatography, magnetic resonance imaging (MRI), and magnetometry (EMMA)—for investigating both static and dynamic articulatory characteristics using a single native speaker of Tamil. Dialectal merger and neutralization phenomena exhibited by the liquids of Tamil are discussed. Comparisons of English /ɹ/ and /l/ with Tamil provide evidence for generality in underlying mechanisms of rhotic and lateral production. The articulatory data justify the postulation of a class of rhotics and a class of laterals in Tamil, but do not provide evidence in favor of a larger class of liquids. Such a superclass appears to have largely an acoustic basis. © *1999 Acoustical Society of America.* [S0001-4966(99)03809-6]

PACS numbers: 43.70.Aj [WS]

INTRODUCTION

Tamil, a Dravidian language of Southern India, is unusual among the world's languages in that many of its dialects have five contrastive liquid consonants (Christdas, 1988, and references cited therein). An accurate articulatory and acoustic characterization of these sounds has been elusive. In this paper, our goal is twofold. First, this work provides a novel use of multiple technologies in speech production research in order to provide a detailed description of the articulatory geometry, kinematics, and acoustic characteristics of these liquids. We have pursued the combined use of multiple methodologies with a single speaker—magnetic resonance imaging (MRI), magnetometry in the form of the electromagnetic midsagittal articulometer (EMMA), static palatography, and acoustic analysis and modeling. This effort continues the exciting recent advances in the use of imaging in speech production research. When combined with more established tools in speech production studies, imaging technology can help identify which aspects of vocal tract behavior are of linguistic significance.

The second goal of this paper is a linguistic one. Liquids have long been recognized as difficult to study, in part because of the diversity of forms these articulations take. Tamil provides a particularly complex set of liquids, including retroflex and nonretroflex articulations. Phonetic study of Tamil thereby provides a unique opportunity to add to the linguistic body of knowledge regarding liquid sounds. This paper contributes to an explicit description of the five liquids of Tamil in the articulatory and acoustic domains, and attempts to identify the linguistically significant aspects of each sound.

The vocal tract geometry of these liquid articulations has been briefly outlined by Narayanan *et al.* (1996). The present study presents a more in-depth description of the articulatory geometry by providing information on the kinematics and articulatory-acoustic relations of these five consonants. It is hoped that by combining, within the same speaker, three-dimensional information available from static MRI with midsagittal kinematic information provided by magnetometry, a more comprehensive understanding can be obtained of the articulatory mechanisms involved in producing this complex system of linguistic contrast.

Advanced technologies such as MRI and magnetometry now enable detailed investigations of complex speech sounds such as liquid consonants. Until now, such sounds have resisted fully satisfactory articulatory descriptions. Each of these techniques has its advantages and disadvantages. MRI scans require artificial prolongation of the sound but provide information on the shape of the vocal tract not obtainable by other methods. Static palatography measures only the aggregate articulatory contact throughout an utterance. Nonetheless, this technique does show fairly precisely which part of the tongue makes contact with which part of the palate. Magnetometry recordings provide valuable dynamic information but are restricted to tracking just a few points along the midsagittal plane. In spite of their respective shortcomings, when combined, the articulatory data available from all three techniques enable us to obtain an increased understanding of vocal tract and tongue shaping mechanisms.

The five liquids of the relevant Tamil dialects are voiced. Two are described as rhotics and two as laterals (e.g., Christdas, 1988). The fifth has been variously described, sometimes as a rhotacized lateral (Balasubramanian, 1972; Christdas, 1988, and references cited therein). This liquid is placed among the rhotic group in the discussion below. The decision was based on the fact that like other rhotic sounds, [ɻ] involves central airflow. Laterals, by contrast, exhibit airflow along the sides of the tongue. Throughout this paper,

TABLE I. Symbols used to identify the five Tamil liquids.

IPA symbol	Description	Romanized orthography
[l̪]	dental l	l
[ɭ]	retroflex 1	L
[r]	pre-alveolar r	r
[r̠]	post-alveolar r	R
[ɻ]	palatal r	zh

the IPA symbols for these liquids proposed by Narayanan *et al.* (1996), based largely on MRI analyses of their geometric tongue shapes, have been adopted. The five liquids are identified then as in Table I.

In the report below, the results of three experiments designed to investigate the articulation of these Tamil liquids are presented. The first two experiments use MRI and static palatography data collected on two different days in 1995 for a single speaker—MRI at Cedars-Sinai Medical Center (Los Angeles, CA) and palatography at the UCLA Phonetics Laboratory. The third experiment reports data collected for the same speaker in 1996 using the EMMA magnetometry system (Perkell *et al.*, 1992) at Haskins Laboratories (New Haven, CT). Thus all the results reported here are based on a single experimental subject, SN (the first author). The static articulatory geometry of the Tamil liquids is described in Sec. I on the basis of the structural MRI and palatography. Section II presents a kinematic analysis of the liquids using magnetometer data.

The information obtained in the experimental work helps illuminate various issues in speech production and linguistic phonetics. In Sec. III, the articulatory-acoustic relations involved in producing these liquids are modeled based on vocal tract dimensions evidenced in the MRI data. The results are compared to the natural speech spectra. It is found that, despite the complexity of these articulations, by using a simple one-dimensional acoustic model and vocal tract data derived from MRI, we are able to establish the basic relations between vocal tract cavities and formant structure. Then, with a comprehensive picture of the articulatory and acoustic characteristics of these sounds in hand, three issues of significance in linguistic phonetics are discussed in Sec. IV. It is postulated that three-dimensional tongue shaping serves to unify articulations within the rhotic group and within the lateral group. Acoustic characteristics, on the other hand, show overlap between these two classes, suggesting that the broader category ''liquid'' has an acoustic basis. Next, a discussion is provided on how information regarding articulatory geometry and kinematics, in addition to a consideration of acoustic characteristics, can be brought to bear in understanding phonological merger and substitution that take place among these sounds. Finally, comparison of the Tamil liquids with the phonetic characteristics of the two liquids of American English is provided.

I. STATIC ARTICULATORY GEOMETRY—MRI AND PALATOGRAPHY FINDINGS

A. Method

1. Subject

MRI and static palatography data were acquired for one native male speaker of the Brahmin dialect (SN, the first author). This subject, who speaks English as a second language, was raised in Madras, India, where he spent the first 20 years of his life. In 1988, he moved to the United States, where he resided at the time of these experiments.

2. Structural MRI

Information about ''static'' vocal tract shapes came from MRI scans (GE 1.5 T scanner) at contiguous 3-mm intervals in the sagittal and coronal anatomical planes. This allowed the construction of three dimensional views of the vocal tract in a computer representation. The subject, in a supine position in the scanner, produced each consonant preceded by /pa/ (i.e., /paC/) and continued sustaining the final consonant for about 13 s, thereby enabling four contiguous image slices to be recorded (3.2 s/slice). The above procedure was repeated until the entire vocal tract region was imaged. (Spectrographic analysis, although not discussed below, indicated that formant values were near steady-state for the sustained utterances.) Details of image acquisition, measurement, and analysis are similar to those given in Narayanan *et al.* (1995). Measurements of vocal tract dimensions and cavity volumes were obtained both from raw image scans and computer reconstructions of the 3-D vocal tract. Area functions reported in this paper (Sec. III B and Appendix B) were obtained by re-sampling the 3-D vocal tract at 0.43-cm contiguous intervals along, and in a plane perpendicular to, the vocal tract midline specified in a midsagittal reference image. The cross-sectional areas were calculated directly by pixel counting.

3. Static palatography

Static palatography was used to register graphically the contact of the tongue with the palate, alveolar ridge, and inner margins of the teeth (Ladefoged, 1957). Carbon powder was coated on the tongue surface prior to speaking, and after articulation the resulting contact patterns on both the tongue and palate were captured with video imaging. This method records any and all palatal areas at which lingual contact occurred. A subset of the words (without a carrier phrase) used for the magnetometry recording (Appendix A) was used for palatography. The resulting (video) palatograms and linguograms provided data that were useful in inferring tongue shapes.

B. Static articulatory geometry—Results

Midsagittal MRI scans for the five (artificially sustained) Tamil liquids are shown in Figs. 1–3. Example tongue-palate contact patterns for the Tamil liquids [l̪], [ɭ], and [ɻ] are given in Figs. 1(e), (f), and 3(b), respectively.

1. Laterals

For the laterals, Fig. 1 shows that [l̪] was characterized by tongue-tip contact in the dental region, a somewhat high-posterior tongue body position, and retraction of the tongue root toward the posterior pharyngeal wall [Fig. 1(a)]. There was a flat anterior surface, but the tongue was generally convex. The curved sides of the posterior tongue create the inward lateral compression characteristic of the consonant (cf.

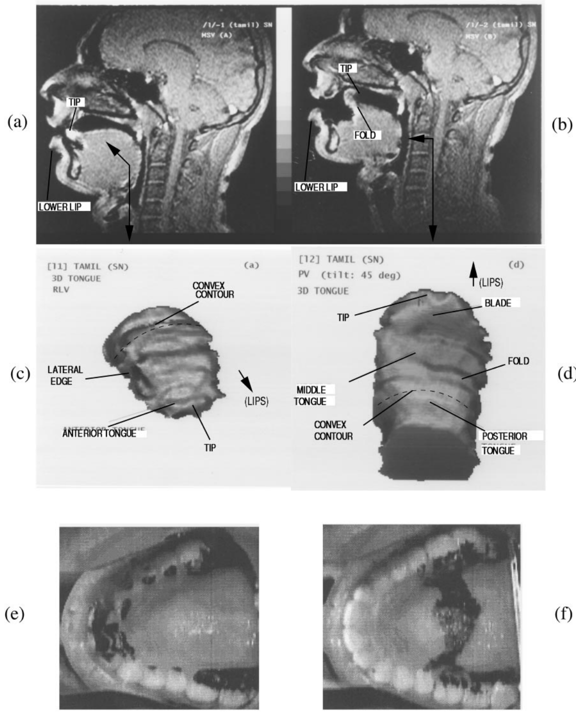

FIG. 1. (a) Midsagittal MR image for [l] (b) Midsagittal MR image for [ɭ]. (c) 3-D tongue shape for [l]. The 3-D tongue is viewed from the side [refer to the view orientation arrow shown in the midsagittal image of panel (a)] and tilted toward the front for better display. The tongue tip appears toward the lower right of the panel. (d) 3-D tongue shape for [ɭ]. The 3-D tongue is viewed from the posterior pharyngeal wall [refer to the view orientation arrow shown in the midsagittal image of panel (b)] and given a forward tilt of 35° for a better view. The tongue tip is toward the top of the panel. (e) Linguapalatal contact for [l], dark region is area of contact, front of mouth is toward the left. (f) Linguapalatal contact for [ɭ] (dark region is area of contact, front of mouth is toward the left).

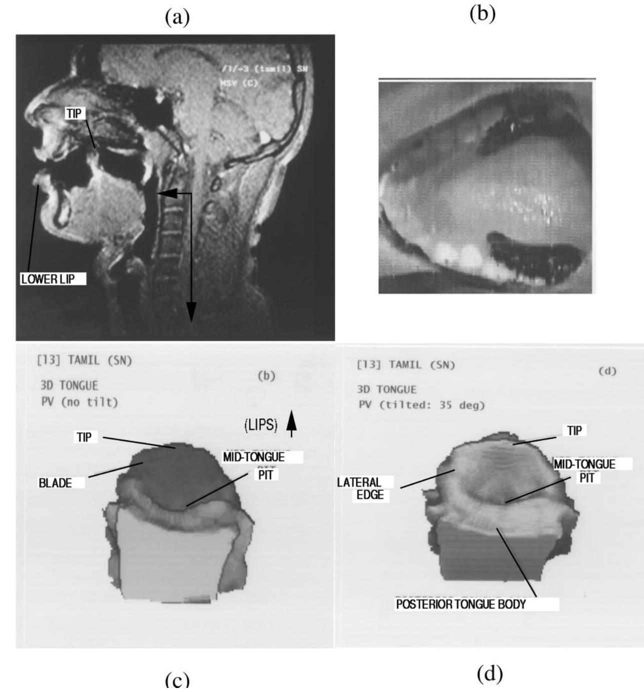

FIG. 3. (a) Midsagittal MR image for [ɻ]. (b) Linguapalatal contact for [ɻ] (dark region is area of contact along the sides of the middle tongue, front of mouth is toward the left). (c) 3-D tongue shape for [ɻ]. The 3-D tongue is viewed from behind, looking in from the posterior pharyngeal wall toward the direction of the lips [refer to the view orientation arrow shown in panel (a)]. The tongue tip is toward the upper middle of panel. (d) Same as in (c), but with a 45° front-to-back tilt of the tongue body to enable a better view of the mid-tongue pit.

Stone *et al.*, 1992; Narayanan *et al.*, 1997). Studying the tongue-palate contact by means of palatography in conjunction with the midsagittal MR images provided further important information. [l] was apical, characterized by medial tongue-tip closure at and behind the central incisors and lateral contact in the postpalatal/velar region (starting near the first molar). Although these patterns suggest lateral airflow paths in the anterior region, prediction of actual cross-sectional tongue shapes and area functions is not straightforward; midsagittal and tongue contact information alone is insufficient.

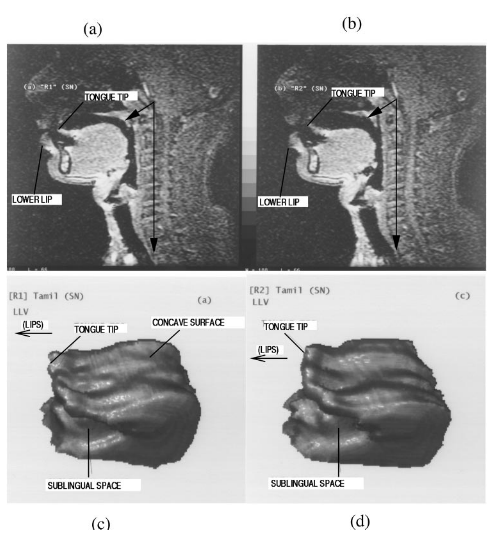

FIG. 2. (a) Midsagittal MR image for [r]. (b) Midsagittal MR image for [r̠]. (c) 3-D tongue shape for [r] (tongue tip toward the left of panel). (d) 3-D tongue shape for [r̠] (tongue tip toward the left of panel).

The anterior tongue body for [ɭ] [Fig. 1(b)] was drawn upward and well inside the oral cavity, with the medial tongue occlusion appearing in the palatal region. The anterior tongue body was flat and raised upward while the posterior tongue body was convex. [ɭ] was subapical with contact made along the edge of the underside of the tongue in the palatal region. It should be noted that [ɭ] in syllable-initial cases is realized as a flap, and often may not involve complete (subapical) palatal contact in fluent speech. In cases where there was complete linguapalatal closure for [ɭ], such as in syllable final position, the anterior contact pattern was more extensive (laterally) when compared to [l].

2. Rhotics

For the rhotics, the overall midsagittal tongues shapes for [r] and [r̠] were very similar (Fig. 2). The tongue-tip constriction for [r] was in the prealveolar region. The tongue surface contour was slightly concave or flat and had lateral bracing in the palatal region. Lingua-palatal contact showed no medial closure. The post alveolar [r̠] had a midsagittal tongue shape similar to [r], but the narrowest tongue-tip constriction was more posterior. The posterior tongue body for [r̠] was somewhat lower than for [r]. The tongue-palate contact patterns obtained by palatography for [r] and [r̠], which are both apical, were not very distinct. In both cases, lateral linguapalatal bracing in the palatal region played a role in tongue shaping.

Lastly, for [ɻ], the anterior tongue body [Fig. 3(a)] was drawn upward and well inside the oral cavity. The narrowest tongue constriction appeared in the palatal region, although the exact location was inconsistent, as was demonstrated by the magnetometer data (see Sec. II). There was no medial linguapalatal contact and central airflow occurred. In addition, there was lateral contact with the tongue body middle in the palatal region (extending for about 1 cm). Crucially, the upward raised and inward pulled anterior tongue position produced a pitlike cavity in the middle of the tongue body that was supported by bracing of the sides of the mid-tongue region against the palate [see Fig. 3(d)]. The posterior tongue had no bracing and was somewhat flat. This liquid was strikingly distinguished from the others by the pitted tongue shape and a correspondingly greater back-cavity volume, the significance of which will be discussed in Sec. III B.

II. ARTICULATORY KINEMATICS—QUANTITATIVE MAGNETOMETRY FINDINGS

A. EMMA method

1. Stimuli

This investigation of the production characteristics of the Tamil liquids focused on the kinematic behavior of the tongue tip. The tongue tip is the articulator that creates the narrowest constriction for all of the liquids. The stimuli included each of the five liquids in the following contexts: /$kaCi, paCi, vaC, aCai, paCam$/ where C was {[l], [ɭ], [r], [r̠], [ɽ]}. Because three of these stimuli were nonsense words, three additional meaningful words with parallel segmental structure were added to supplement the list. This yielded a total corpus of 28 words. These words were randomized and presented in the carrier phrase *''Andha vakyam __ perusu''* ⟨*The utterance __ is big.*⟩ Ten repetitions of this randomized list were recorded. These words are shown in Appendix A as they were presented to the subject. In all, 280 sentences were recorded.

2. Subject and data collection

The EMMA magnetometer system (Perkell *et al.*, 1992) was used to track the movement of the articulators. These data were acquired from the same speaker (see Sec. I A 1) who recorded for the MRI and static palatography experiments, i.e., a native male speaker of the Brahmin dialect (SN). This experiment was part of a longer magnetometer recording session, and was the second of three recordings in that session.

The EMMA magnetometer system was used to transduce the horizontal (x) and vertical (y) movements of small coils attached to the articulators in the midsagittal plane. The technical specifications of the EMMA magnetometer system are outlined in Perkell *et al.* (1992) (see also Gracco and Nye, 1993; Löfqvist, 1993). Single transducers were placed on the nose, upper and lower gumline (maxilla and jaw, respectively), upper and lower lips at the vermilion border, tongue tip, and three transducers were placed on the tongue body. The EMMA data were sampled at 625 Hz after low-pass filtering at 200 Hz before voltage-to-distance conversion. After voltage to distance conversion (with a filter cutoff of 17 Hz), correction for head movement (using the nose and maxillary reference transducers), and rotation to the occlusal plane, the position signals were subject to 25-point smoothing by a triangular filter.

3. Data analysis

The measurements made in this experiment were of the spatiotemporal behavior of the transducer placed on the tongue tip (approximately 7 mm, with the tongue somewhat extended, from the tongue-tip apex on the superior surface).

a. Signal analysis. Horizontal (x) and vertical (y) position signals for the tongue-tip transducer were used to calculate the tangential velocity of the tongue tip according to the following formula:

$$tvel=\sqrt{((\dot{x})^2+(\dot{y})^2)},$$

where $tvel$ = tangential velocity of the tongue-tip transducer, $\dot{x}$ = velocity in the x-coordinate of the tongue-tip transducer, $\dot{y}$ = velocity in the y-coordinate of the tongue-tip transducer. This signal was also smoothed at 25 points.

The beginning, extremum, and end of the production of the liquid consonant were defined by algorithmically identifying minima in the tangential velocity signal using the HADES signal analysis program (Rubin, 1995). The time and tongue-tip x- and y-positions at each of these points were recorded. [See Löfqvist *et al.* (1993) for a description of the use of tangential velocity in the segmentation of magnetometer signals.] Additionally, for each opening and closing movement, time and magnitude of the peak tangential velocities were collected. Finally for each constriction formation (interval between beginning and extremum) and constriction release (interval between extremum and end), the pathlength and average curvature were calculated. Pathlength is the actual (midsagittal) distance traveled by the transducer, and is calculated by summing the consecutive Euclidean distances between each sample. Curvature is indicative of the direction of movement with negative values for clockwise movement and positive values for counterclockwise movement, assuming that the subject is facing to the left. [See Löfqvist *et al.* (1993) for a more extensive discussion of the use of curvature information in the analysis of EMMA data.] This calculation was made according to the following formula:

$$\overline{curvature}=\frac{\Sigma((\dot{x}\ddot{y}-\ddot{x}\dot{y})/tvel^3)}{constriction\ \ interval},$$

where $\overline{curvature}$ is the average curvature value over constriction formation (or release), $\dot{x}$ (or $\dot{y}$) is the x (or y) component velocity, $\ddot{x}$ (or $\ddot{y}$) is the x (or y) component acceleration, $tvel$ is the tangential velocity, and *constriction interval* is the duration of the constriction formation (or release). Figure 4 shows an example of measurements made for a token of [palam]. A movement token was excluded if multiple velocity minima occurred at the movement's extremum or if multiple velocity maxima occurred during a single constriction

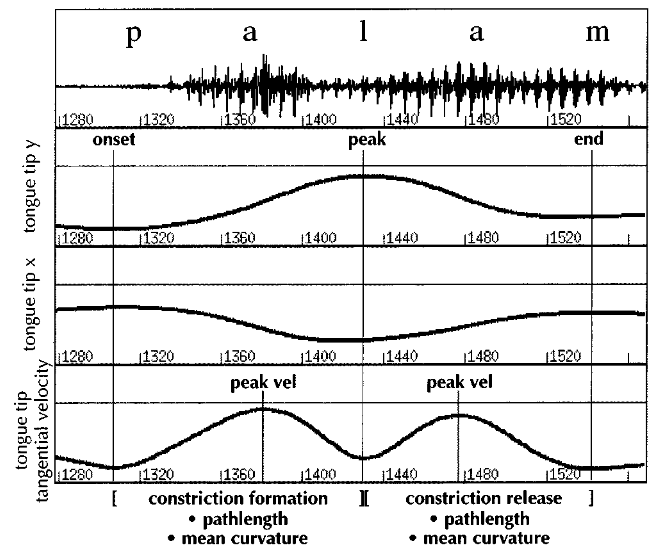

FIG. 4. A sample token of EMMA data indicating the measurements made for experiment 3.

formation or release. Such exclusions were rare, amounting to 21 tokens (out of 280 stimuli). Of these, 17 were word-final liquids, including all 10 tokens of the word final [ɭ].[1] Lastly, the automated algorithm for calculating curvature failed for 13 tokens, 2–4 tokens of each liquid type.

b. Quantitative analysis. The complete list of kinematic variables considered in the statistical analysis is shown below. (Recall that constriction beginning, extremum, and end points are defined by the tangential velocity minima; that constriction formation is defined as the interval between beginning and extremum; and that constriction release is defined as the interval between extremum and end.)

(a) the tongue-tip *y*-position at extremum constriction;
(b) the tongue-tip *x*-position at extremum constriction;
(c) peak tangential velocity for constriction formation and release;
(d) pathlength for constriction formation and release;
(e) average curvature for constriction formation and release;
(f) duration of constriction formation and release;
(g) time from onset to peak constriction velocity;
(h) proportional time from beginning to peak constriction velocity (i.e., time to peak velocity/duration of constriction formation).

These measurements reflect the duration and magnitude of the formation and release of the liquid articulations and help illuminate certain aspects of the intragestural dynamics.

Three statistical analyses were conducted using a $p \leq 0.05$ criterion for significance. The first analysis was a two-factor ANOVA with the factors LIQUID (dental [l], retroflex [ɭ], prealveolar [r], postalveolar [r̠], palatal [ɹ̣]) and VOCALIC CONTEXT (a_a, a_i, a_ai, a_#). For this analysis, *post hoc* Scheffé's S-tests (Scheffé, 1953) were used to test *post hoc* comparisons among the liquids. (Because of the many possible crossings of the two factors, discussion of vocalic context effects are left for the second analysis.) This analysis examines all the dependent variables (a)–(h) listed above. The second analysis was a two-factor ANOVA testing for effects of LIQUID and VOWEL HEIGHT (lowV_lowV and lowV_hiV). Main effects of contextual vowel height are reported, as well as any crossover interactions between LIQUID and VOWEL HEIGHT. The final analysis was a two-factor ANOVA testing for effects of LIQUID and WORD POSITION (word final and intervocalic). (Note that there are generally many fewer word final tokens than intervocalic tokens, and no data for the retroflex [ɭ] could be included.) Main effect of WORD POSITION and any crossover interactions with LIQUID are reported. The final two analyses examined only a subset of the dependent variables.

B. Articulatory kinematics—Results

1. Analysis one—Main effects of liquid identity

There was a main effect of liquid on both peak *x*-position $[F(4,241)=460.774,\ p=0.0001]$ and peak *y*-position $[F(4,241)=1937.996,\ p=0.0001]$. *Post hoc* tests showed all the liquids to differ significantly in peak tongue-tip *x*-position, and all except the dental [l] and post alveolar [r̠] to differ significantly in peak tongue-tip *y*-position.[2] The five liquids were highly differentiable in *x*-*y* space by their tongue-tip positions at peak constriction. The dental [l], prealveolar [r], and postalveolar [r̠] moved progressively back in the *x*-dimension, with little difference in the *y*-dimension. The palatal [ɹ̣] and retroflex [ɭ] were considerably back and somewhat higher than the other liquids. The palatal [ɹ̣] showed the most variability in *y*. This variability in tongue-tip position reflected a greater propensity to coarticulation with neighboring vowels. The variability in [ɭ] was less than in [ɹ̣] ([ɭ] showed some fronting in the *x*-dimension in the /a_i/ context). The relative *x*,*y*-positions for the liquids are shown in Fig. 5. Recall that examination of static MRI and palatography data outside the midsagittal plane demonstrated that the palatal [ɹ̣] and the retroflex [ɭ] also differed in that the former had tongue side bracing that the latter lacks. While the tongue sides were braced, the tongue tip was free, giving rise to an expectation of positional variability on the part of the tongue tip. This expectation was borne out by the magnetometer findings—observe the greater scattering of the *y* tongue-tip position for [ɹ̣] in Fig. 5.

Apart from the positional characteristics of liquid production, dynamic characteristics such as the constriction formation and release velocities also provided useful information. The constriction formation peak velocities were significantly affected by liquid identity $[F(4,241)=127.1307,\ p=0.0001]$ with all liquids differing from one another except the dental [l] and the palatal [ɹ̣]. The retroflex [ɭ] and the postalveolar [r̠] had the highest constriction formation peak velocities, and these are the sounds that are typically described as flap and tap articulations, respectively. The constriction release peak velocities were also significantly affected $[F(4,241)=1623.2642,\ p=0.0001]$ and differed for all liquids except the dental [l] and the postalveolar [r̠]. These velocities were much higher for the two backmost articulations—the palatal [ɹ̣] and the retroflex [ɭ]—with the backer of the two, i.e., the retroflex [ɭ], having the highest peak release velocities. The backmost [ɭ] had about three

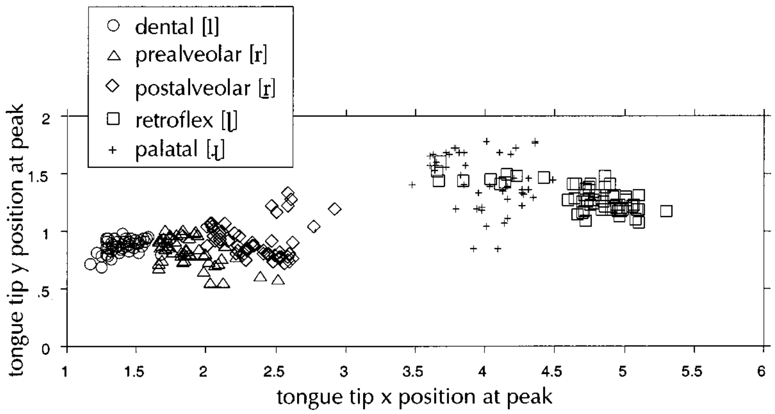

FIG. 5. Tongue-tip *x*- and *y*-positions with respect to the occlusal plane at *y*-peak for the five liquids.

times the release velocity of the fronter three articulations, [l], [r], and [r̠], which differed only minimally among themselves. The slightly fronter [ɻ] had about two times the release velocity of [l], [r], and [r̠]. Thus more posterior tongue-tip constriction position correlated with increased release velocity.

Constriction formation duration and pathlength exhibited similar patterns [$F(4,241)=46.1668$, $p=0.0001$; $F(4,241)=176.8743$, $p=0.0001$]. *Post hoc* tests showed that constriction formation duration is shortest for fronter articulations—the dental [l], prealveolar [r], postalveolar [r̠]—and longest for the backer ones—palatal [ɻ] and the retroflex [ɭ]. Constriction formation pathlength was shortest for the prealveolar [r], next shortest for dental [l], intermediate for the postalveolar [r̠], longer for the palatal [ɻ], and longest for the retroflex [ɭ]. Here, greater constriction formation pathlengths and durations tend to correlate with posterior tongue-tip position.

Release duration and pathlength displayed similar patterns [$F(4,241)=115.0354$ $p=0.0001$; $F(4,241)=1444.7914$, $p=0.0001$]. Just like constriction formation duration, release duration was shortest for fronter articulations—the dental [l], prealveolar [r], postalveolar [r̠]—and longest for articulations further back—palatal [ɻ] and the retroflex [ɭ]. Release pathlength was shortest for the dental [l] and prealveolar [r], slightly longer for the postalveolar [r̠], longer for the palatal [ɻ], and longest for the retroflex [ɭ]. Overall, the constriction and release duration and pathlength data follow the general pattern of the-farther-the-longer behavior that has been found to be typical of both speech and limb movements, whereby durations tended to be longer for movements with larger displacements (e.g., Kelso *et al.*, 1985; Ostry and Munhall, 1985; Saltzman *et al.*, in press).

Recall that constriction formation curvature refers to the direction of tongue-tip movement. This measure was significantly affected by liquid identity [$F(4,228)=59.2735$, $p=0.0001$] (see Fig. 6). It was positive with low variability for the retroflex [ɭ] and palatal [ɻ]. This means that the two high back articulations [ɭ] and [ɻ] had counterclockwise movements (head facing to the left). In other words, the *x*-component peak was attained before the *y*-component peak. Curvature was negative for [r] and [r̠], with [r̠] exhibiting low variability and [r] exhibiting moderate variability. For the dental [l], this measure tended to be negative but quite variable, with many tokens having a near zero value. *Post hoc* tests indicated that the positive-curvature articulations differ significantly from the negative-curvature articulations.

Liquid identity also affected release curvatures [$F(4,228)=26.5673$, $p=0.0001$]. Positive values for the retroflex [ɭ] and negative values for postalveolar [r̠] were observed. It was fairly consistent that release curvature was slightly positive with low variability for [ɻ] and slightly negative for prealveolar [r]. It was quite variable for the dental [l], including many positive and negative values. The patterns for curvature can be summarized as follows. The dental [l] was formed with a straight (uncurved) or slightly clockwise movement and may be released in either a clockwise or counterclockwise direction. The retroflex [ɭ] and palatal [ɻ] were formed and released in the counterclockwise direction, i.e., back-to-front. The [r] and [r̠] were formed and released with a basically clockwise direction, front-to-back. Note that

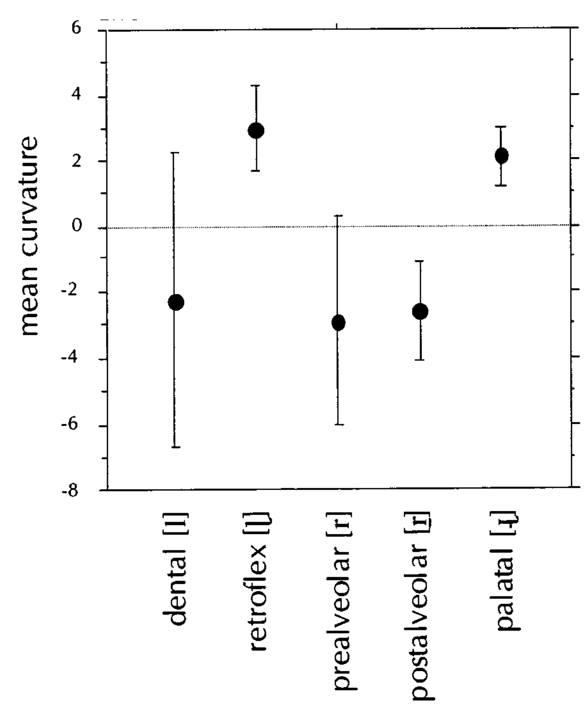

FIG. 6. Mean constriction formation curvature for the five liquids with one standard deviation error bars.

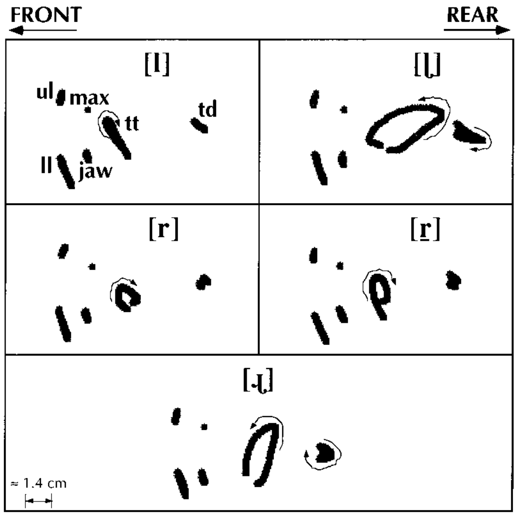

FIG. 7. Sample position trajectories for the tongue tip, with the upper lip, lower lip, maxilla, jaw, and tongue dorsum shown for reference, for tokens of each of the five liquids in the [a_a] context. Arrows indicate the direction of movement of the tongue tip, and where necessary the tongue dorsum. The trajectories are displayed for the interval between the points of minimum tongue-tip height preceding and following the constriction.

while the tongue tip for palatal [ɻ] was quite variable in the *x*,*y*-position, it was remarkably consistent in curvature. Figure 7 provides a qualitative visual aid for observing the overall location and direction of tongue tip movement for each liquid.

Finally, consider the time from the onset of constriction formation to peak velocity, as well as this interval normalized for the duration of the constriction formation interval. The latter is a measure of the skewness of the velocity profile. These variables provide insight into the temporal dynamics underlying the constriction formation. These variables will be referred to as time to peak velocity and proportional time to peak velocity. These variables are of specific interest in considering the contextual effects covered in the following two sections, but some differences do exist among the liquids independent of context [$F(4,241) = 14.7912$, $p = 0.0001$ for time to peak velocity and $F(4,241) = 52.0319$, $p = 0.0001$ for proportional time to peak velocity]. *Post hoc* tests showed the retroflex [ɭ] to have a longer time to peak velocity than the other liquids. The postalveolar [r̠] was also found to have a longer time to peak velocity than dental [l]. For proportional time to peak velocity, *post hoc* tests found almost all pairwise comparisons to differ significantly. Peak velocity occurs proportionally earlier for the palatal [ɻ], intermediate for the [l] and [ɭ], and latest for the [r] and [r̠].

2. Analysis two—Main effects of contextual vowel height

In this analysis the stimuli were assigned to two vowel height groupings. The Lo_Lo group included the *aCai* and *paCam* words and the Lo_Hi group included the *kaCi* and *paCi* words. Note that these groupings are a function of *following* vowel height. (Interesting effects on the liquid articulations due to preceding vowel height are likely to exist; unfortunately, the stimuli did not allow us to investigate these effects because in all cases the liquid in question was preceded by the vowel [a].) Two-factor ANOVAs with LIQUID and VOWEL HEIGHT as factors were conducted. Below are described the main effects of vowel height on (1) peak *x*- and *y*-positions, (2) constriction formation and release durations, and (3) constriction formation and release pathlengths.

Small but significant effects of following vowel height existed for peak positions [$F(1,217) = 49.8508$, $p = 0.0001$ for *x*-position, and $F(1,217) = 121.1377$, $p = 0.0001$ for *y*-position] such that the Lo_Hi context had fronter and higher tongue-tip positions at peak for all liquids. These differences were small for [l], and relatively large in the *y*-dimension for [ɻ]. No significant effect was found for pathlength or release duration. The constriction formation duration is shorter [$F(1,217) = 9.0261$, $p = 0.003$] for the Lo_Hi context, especially for the nonfront liquids.

3. Analysis three—Main effects of word position

Byrd and Saltzman (1998) have demonstrated that increased absolute (and for some speakers, proportional) time-to-peak velocity are informative dynamic ''signatures'' of phrase-final lengthening. (They relate this to a lowering of the stiffness parameter in a critically damped mass-spring gestural model.) This present analysis investigated whether these articulatory signatures of lengthening existed for word-final liquids. In this analysis the stimuli were assigned to two groupings: intervocalic and word-final. Note that for the palatal [ɻ] this included only six tokens, for the postalveolar [r̠] this included only seven tokens, and no tokens of retroflex [ɭ] are included. For this reason the results below, while robust, must be considered preliminary. Two-factor ANOVAs with LIQUID and WORD POSITION as factors were conducted. Tests for main effects of word position on constriction formation, release duration, and pathlength, as well as absolute and proportional time-to-peak velocity are presented below. These dependent variables were chosen for examination in the expectation that they would be the most likely to exhibit positional effects such as word-final lengthening.

Word position had no significant effect on either constriction release duration or pathlength. However, word position did have a significant effect on both constriction formation duration and pathlength. Constriction formation duration was longer word-finally for all liquids [$F(1,194) = 141.903$, $p = 0.0001$], and pathlength was longer word-finally [$F(1,194) = 175.4454$, $p = 0.0001$] for [l], [r], and [r̠] but not for [ɻ]. Finally, proportional time to peak velocity was longer word-finally [$F(1,194) = 28.0729$, $p = 0.0001$] for all the liquids and absolute time-to-peak velocity was longer word-finally [$F(1,194) = 30.2707$, $p = 0.0001$] for [l], [r], and [r̠] but again not for [ɻ]. While it is conceivable that the speaker employed a phrase boundary after the target word, indicating phrasal rather than word level lengthening, the experimenters, having listened to the sentences, believe this to be unlikely. It is more likely that these data contain instances of word-final lengthening.[3]

III. ARTICULATORY—ACOUSTIC RELATIONS

In this section, a description of the acoustic characteristics of Tamil liquid consonants and an investigation of the basic underlying articulatory-acoustic relations are provided. As seen in the previous sections, Tamil has lateral and rhotic approximants, occurring as both retroflex and nonretroflex. In general, both laterals and rhotics tend to have a formant structure similar to that of vowels (Ladefoged, 1982). The lateral sounds of the world's languages exhibit a wide variety of articulation and of concomitant acoustic characteristics (Ladefoged and Maddieson, 1996). Both lateral consonants in Tamil are voiced lateral approximants. Ladefoged and Maddieson (1996) summarize the general acoustic characteristics of voiced lateral approximants as follows: an $F1$ rather low in frequency, an $F2$ that may have a center frequency anywhere within a fairly wide range depending on the location of the occlusion and the profile of the tongue, an $F3$ with a relatively strong amplitude and high frequency, and possibly several closely spaced formants above the frequency of $F3$.

There is an even wider range of articulatory variation among the rhotic sounds of the world's languages. Rhotic sounds have been associated with lowered third formant frequency (Lindau, 1985) based mainly on data from English (e.g., Delattre and Freeman, 1968; Espy-Wilson, 1992). (See for examples of exceptions, such as in uvular and dental r-sounds, Ladefoged and Maddieson, 1996, pp. 244–245.) The acoustic correlate of the retroflex consonantal posture is the general lowering of the third and fourth formants (Ladefoged, 1982). More specifically, Fant (1968) associates retroflex modification of alveolar sounds to the lowering of $F4$ frequency so that it comes close to $F3$, and the retroflex modification of palatal sounds to the lowering of $F3$ frequency so that it comes close to $F2$.

A. Acoustic characteristics of Tamil liquids

Sample acoustic spectra of the five Tamil liquids are shown in Fig. 8. These acoustic spectra were obtained from /paC/ utterances recorded in a quiet sound booth by subject SN. The data were directly digitized onto a SUN Workstation at 32 kHz and later down-sampled to 8 kHz. The final liquid consonant in these utterances was artificially sustained in a procedure similar to that followed during the MRI experiments. DFT and 14th-order LPC spectra (Fig. 8) were calculated from 25-ms Hanning-windowed segments taken at approximately 50 ms into the production of the liquid. Formant values of the sustained liquids were found to be consistent across repetitions.

All five liquids were characterized by an $F1$ in the 400–450 Hz range. The dental [l] had a clearly defined $F2$ at 1200 Hz, a relatively broad spectral peak signifying $F3$ around 2400 Hz, and an $F4$ peak around 3850 Hz. $F2$ and $F3$ of the retroflex lateral [ɭ], on the other hand, appeared close to each other, around 1460 and 1800 Hz. $F4$ and $F5$ for [ɭ] were around 2500 Hz and 3600 Hz, respectively. In addition, there appeared to be a spectral zero around 3500 Hz for [l] and around 3300 Hz for [ɭ]. It may be that this zero was responsible for the decrease in the prominence of $F4$ and $F5$. In general, these formant frequency values for this subject's laterals are comparable to the data from a male Tamil speaker reported by Ramasubramanian and Thosar (1971): average $F1$, $F2$, and $F3$ frequency values (in Hz) of

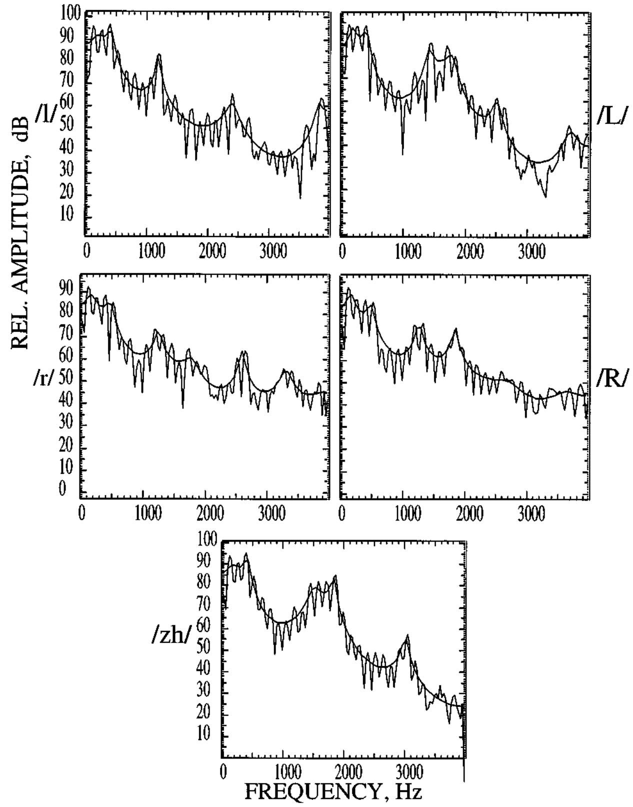

FIG. 8. Sample acoustic spectra of five Tamil liquids (DFT with an LPC overlay).

300, 1300, and 3000, respectively, for /l/; and 280, 1450, and 1600, respectively, for /ɭ/ (both produced in inter-vocalic position).

The acoustic characteristics of the prealveolar and the postalveolar rhotics were very similar to one another except for a slight difference in $F3$ values: 1700 Hz versus 1850 Hz, respectively. In general, the average difference between the $F3$ values of the [r] and [r̠] was about 100 Hz. $F2$, $F4$, and $F5$ are around 1200, 2600, and 3600 Hz for both [r] and [r̠].

The low-frequency acoustic characteristics of the retroflex approximant /ɻ/ were strikingly similar to those of the retroflex lateral [ɭ]: $F2$ and $F3$ were close to each other, around 1500 and 1850 Hz, respectively. $F4$, however, was around 3000 Hz, about 500 Hz higher than the $F4$ of [ɭ]. No significant spectral peaks or valleys were evident above 3000 Hz.

B. Articulatory-acoustic relations in Tamil liquids

In this section, the basic articulatory-acoustic relations in Tamil liquids are outlined using vocal tract dimensions derived from MRI data. Figure 9 shows the area functions for the five Tamil liquids of subject SN. The numerical area-function values are given in Appendix B. For the analysis presented in this section, planar acoustic wave propagation in the vocal tract was assumed. Furthermore, source-filter separability was assumed, and the effects of the vocal tract bend and vocal tract losses were ignored. Under these assumptions, the vocal tract cavities can be roughly approximated as concatenated uniform cylindrical tube sections. As a further approximation, only averaged areas of the vocal tract cavities

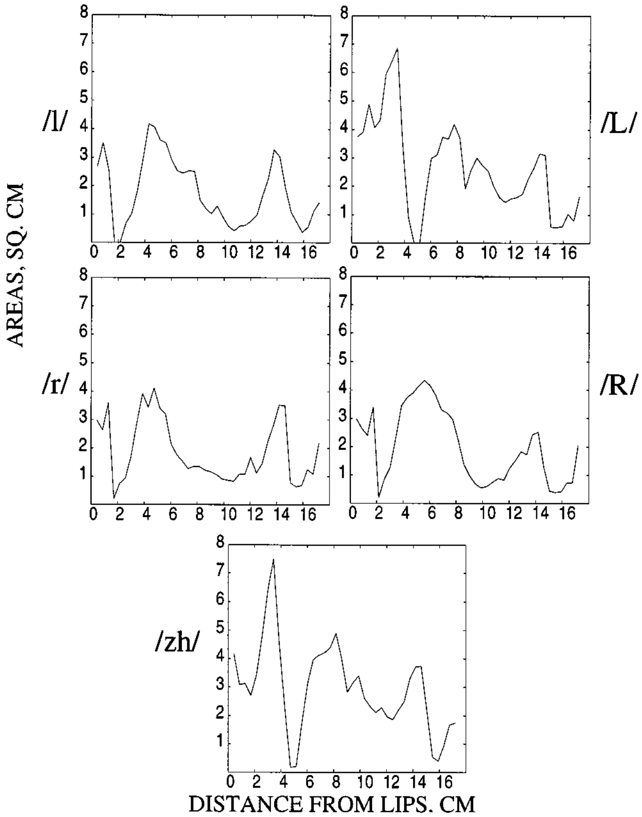

FIG. 9. MRI-derived area functions for five Tamil liquids.

to the front and back of the oral constriction were considered. The following abbreviations are used: L_b and A_b refer to back-cavity length and area; L_f and A_f refer to front-cavity length and area; L_c and A_c refer to constriction length and area. L_s and A_s refer to sublingual cavity length and area (for rhotics) or side-cavity length and area (for laterals). Although a somewhat oversimplified approximation, the analysis of such tube models is aimed at providing insights into the origin of the poles and zeroes of the vocal tract transfer function. [Acoustic modeling experiments wherein area functions of Tamil liquids are directly input to an articulatory synthesizer are reported in Narayanan and Kaun (1999).] The analysis presented here followed the general acoustic modeling principles proposed in Flanagan (1972) and Stevens (1998).

The tube dimensions obtained from the MRI data for each sound (Fig. 9) are listed in Table II. For the laterals, the

TABLE II. Vocal tract tube dimensions estimated from MRI-derived area functions. L_b and A_b refer to back-cavity length and area, L_f and A_f to front-cavity length and area, and L_c and A_c to the constriction length and area. L_s and A_s refer to the sublingual length and area (for [r] and [r̠]) or the lateral channel length and area (for [l] and [ɭ]).

Liquid	L_b (cm)	A_b (cm^2)	L_f (cm)	A_f (cm^2)	L_s (cm)	A_s (cm^2)	L_c (cm)	A_c (cm^2)
[l]	14.62	1.83	1.72	3.3	2.5	2.5	0.86	0.5
[ɭ]	11.61	2.4	4.73	4.75	2.58	2.5	0.86	0.4
[r]	14.6	1.89	1.72	1.89	2.8	0.85	0.86	0.2
[r̠]	14.19	2.02	2.15	2.02	2.15	1.26	0.86	0.2
[ɻ]	11.61	2.88	4.73	2.88	-	-	0.86	0.18

TABLE III. Average frequency values of the first four formants (in Hz) for the five Tamil liquids. Obsv. refers to values measured from spectra of natural speech and Est. refers to values estimated by the tube models (Sec. IV B).

	$F1$		$F2$		$F3$		$F4$	
Liquid	Obsv.	Est.	Obsv.	Est.	Obsv.	Est.	Obsv.	Est.
[l]	400	480	1200	1180	2400	2360	3850	3540
[ɭ]	400	540	1460	1480	1800	1822	2500	2460
[r]	460	507	1200	1200	1700	1765	2600	2400
[r̠]	460	507	1200	1233	1850	1935	2600	2466
[ɻ]	450	433	1500	1485	1850	1822	3025	2970

areas of both the side channels were combined and modeled as a single channel. L_c for the laterals was taken to be the length of the medial tongue occlusion, while A_c was the average combined side channel area over the occlusion region. For the rhotic sounds, the tongue-tip constriction region, defined by the minimum area in the area function, was taken to be approximately two area function sections, that is, 0.86 cm. Once the constriction region was defined, the front- and back-cavity lengths were measured, respectively, from the lip opening to the constriction-region beginning and from the glottis to the constriction-region ending. With the aid of cross-sectional MRI data, the side-cavity length L_s for the laterals was defined to be the length along which a space existed between the sides of the convex tongue surface contour and the oral cavity wall. The sublingual length L_s for the alveolar rhotics was defined to be the oral cavity length for which a distinct airspace area under the tongue surface was measurable.

The vocal tract resonance frequency values were estimated from the tube model and were compared to the measured values obtained from the subject's natural speech. These results are summarized in Table III. Note that for all the calculations reported below, the speed of sound in air, c, equals 34 480 cm/s.

$F1$ for all the liquids can be attributed to the natural frequency of the Helmholtz resonator formed by the back cavity and the constriction created by the anterior tongue. The estimated Helmholtz resonance values $[(c/2\pi) \times \sqrt{A_c/(L_b^* A_b^* L_c)}]$ ranged between 400 and 500 Hz. In spite of significant differences in back-cavity lengths across the five liquids, differences in the volume of the Helmholtz resonator were relatively minimal. Tongue shaping helped achieve this back volume ''normalization:'' the back-cavity volume in the case of the retroflex sounds was made larger by either concave or pitted surface contour (as in the case of [ɻ]) or a lowered posterior tongue body (as in the case of [ɭ]). On the other hand, the rhotics and the dental [l] had a relatively higher mid- and posterior tongue body height and either a convex contour ([l]) or a less concave contour (rhotics).

In a highly simplified approximation, the vocal tract configuration for the lateral sounds can be modeled by just two tubes representing the back and front cavities that are separated by a constriction. In such a case, the back-cavity resonances $[(N^*c)/2L_b,\ N=1,2,3,....]$ for ([l]) were estimated at 1180 Hz, 2358 Hz, 3540 Hz, etc.; while for [ɭ], they

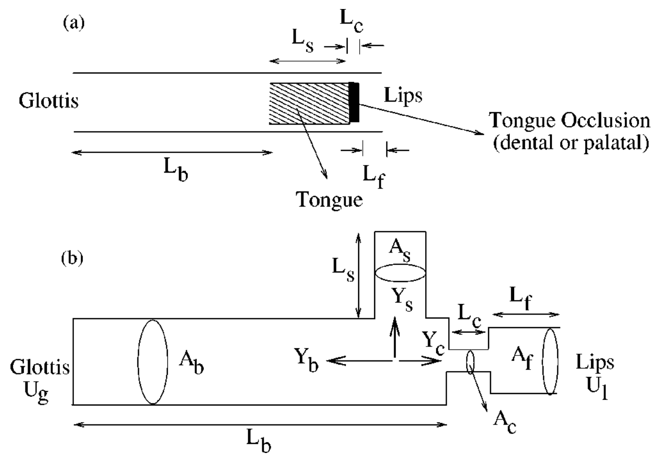

FIG. 10. (a) Schematic of the oral cavity configuration (as viewed looking down from the palate) for the lateral sounds. (b) A tube model approximation for the lateral sounds (see Sec. III for explanation of the various symbols).

were at 1485 Hz, 2975 Hz, 4455 Hz, etc. Frequency of the lowest front-cavity resonance $[=c/4*L_f]$ was above 5000 Hz for [l], while the relatively longer front cavity for [ɭ] yielded a smaller frequency value of around 1820 Hz for the lowest front-cavity resonance. Hence for /l/, $F2$, $F3$, and $F4$ are attributed to the first three back-cavity resonances. For /ɭ/, $F2$ and $F4$ are attributed to back-cavity resonances, while $F3$ is the lowest front-cavity resonance. While these estimated values provide some gross indications of the vocal tract cavity affiliations of the peaks in the natural speech spectra, they are not adequate for explaining the zeroes in the spectrum.

Consider now a more detailed model that includes the effect of the lateral channel [a schematic is shown in Fig. 10(a)]. The corresponding tube model is shown in Fig. 10(b). Stevens (1998) has proposed a similar model for laterals that explicitly includes a side channel. As a result of the presence of lateral channels along the sides of the tongue due to the medial tongue occlusion, a cavity of approximately the length of the lateral channel is created behind the medial tongue occlusion. This cavity extends between the medial occlusion created by the anterior tongue (in the dental region for [l] and the palatal region for [ɭ]) on one end and is open to the oral cavity in the direction of the pharynx. This cavity is modeled as a shunt branch while the flow along the sides of the tongue is combined and modeled as a single channel representing the main airway path. The modified back-cavity length is (L_b-L_s). Assuming that the front and back cavities can be decoupled, the poles of the transfer function U_l/U_g between the volume velocity at the lips, U_l, and at the glottis, U_g, would include the natural resonances of the combined side channel and the modified back cavity and the natural resonances of the front cavity. The zeroes for the transfer function U_l/U_g occur at frequencies for which the acoustic impedance, Z_s, looking into the cavity created as a result of the medial tongue occlusion and side airway branch creation, is zero. If L_s is the length of the uniform tube approximation of this cavity, then the frequency of the lowest zero occurs at $[=c/4*L_s]$.

In summary, the analysis for the Tamil lateral approximants yielded the following results (Table III). For [l], the lowest zero frequency was at 3450 Hz. This zero is at the frequency for which the impedance looking into the side branch is zero. The poles of the transfer function were at 1180 Hz, 2360 Hz, 3540 Hz, and 4720 Hz. Due to the relatively short length of the cavity anterior to oral constriction for the dental [l], there was no contribution to the spectrum from the resonances of the front cavity in the range of interest below 5 kHz (the frequency of the lowest front-cavity resonance, $[=c/4*L_f]$, is around 5 kHz). Approximate analysis suggests that $F1$ is the Helmholtz resonance between the constriction and the back-cavity volume, while $F2$, $F3$ and $F4$ are half-wavelength resonances of the combined back and side cavities.

For [ɭ], the lowest zero frequency was around 3340 Hz. Estimated poles from the cavities behind the oral constriction were at 1485 Hz, 2970 Hz, and 4454 Hz. The lowest front-cavity resonance was at 1822 Hz. Hence the formant frequencies for [ɭ] can be summarized as $F1=540$ Hz, $F2=1480$ Hz, $F3=1822$ Hz, $F4=2460$ Hz, and $F5=3650$ Hz. $F2$, $F3$, and $F5$ are combined back- and side-cavity resonances, while $F3$ is attributed to the front cavity. Compared to [l], $F2$ and $F3$ in [ɭ] were closer to each other mainly due to the longer front cavity resulting from the constriction in the palatal region created by the retroflexed tongue.

As a first approximation, a two cavity tube can be used to model the acoustics of the Tamil rhotic sounds [r] and [r̠]. Notice that the front cavity is modified by a significant (sublingual) area under the raised tongue tip (Fig. 2). As a further approximation, the region in front of the tongue tip constriction can be modeled as a single cavity that extends between the lip opening and the end of the sublingual space. A justification for this approximation comes from the fact that the sublingual opening for the vocal tract configurations of Tamil [r] and [r̠] is relatively large compared to the cross-sectional areas of the sublingual cavity. Under this approximation, the effective front-cavity length is increased by the amount of the sublingual cavity length. This results in an effective front-cavity resonance frequency, $[=c/4*L_f]$, of 1907 Hz and 2004 Hz for [r] and [r̠], respectively. A similar approach wherein the sublingual space is modeled as an extension of the front cavity has been found to produce satisfactory prediction of $F3$ frequencies for American English /r/ (Espy-Wilson *et al.*, 1997). An additional correction for lip rounding (which is not accurately measurable from the MRI data) will further lower the front-cavity resonance by about 100 Hz. The back-cavity resonances for [r] and [r̠], $[(N*c)/2L_b,\ N=1,2,3,....]$, are around 1200 Hz, 2400 Hz, 3600 Hz, etc. In summary (Table III), $F2$ for the rhotics [r] and [r̠] corresponds to the lowest back-cavity resonance (around 1200 Hz). $F3$ corresponds to the lowest sublingual-inclusive front-cavity resonance (about 1800 Hz for [r] and 1900 Hz for [r̠]). $F4$ corresponds to the back-cavity resonance at 2400 Hz.

A more accurate model would include a separate side branch cavity to model the sublingual effect, cf., sublingual models proposed for postalveolar fricatives (Narayanan, 1996), American English /r/ (Espy-Wilson *et al.*, 1997), and ‘‘retroflex /r/’’ (Stevens, 1998). Such a model would also yield a zero in the frequency range of interest (3100 Hz and 4000 Hz for the sublingual dimensions of [r] and [r̲] noted in Table III, respectively). This zero may contribute to lowering the amplitude of the high-frequency formants $F4$ and $F5$, as seen in the spectrum shown for [r̲] (Fig. 8). However, it should be noted that the lack of a clear indication of zeroes in the spectra of voiced sounds is not uncommon, given their harmonic structure, as in the case of the spectrum of [r] in Fig. 8.

Finally, the retroflex approximant /ɻ/ is considered. The front- and back-cavity dimensions are very similar to those of /ɭ/ explaining the similarity in their low-frequency spectral characteristics ($F2$ and $F3$ close to each other at 1485 and 1800 Hz, due to the lowest back- and front-cavity resonances). The only other significant peak around 2975 Hz is attributed to a back-cavity resonance. The lack of significant lateral channels is reflected by the lack of zeros in the high-frequency region (2.5–5 kHz), distinct from the spectrum of /ɭ/.

The formant frequency values estimated from the tube models, assuming decoupled front and back cavities, correspond fairly well with the values measured from the natural speech of subject SN, as shown in Table III. In summary, using a simple one-dimensional acoustic model and vocal tract data derived from MRI, it was possible to establish the basic relations between vocal tract cavities and formant structure.

IV. DISCUSSION

A. Regarding the significance of tongue shaping

Our data lead to an interesting conclusion: tongue shape mechanisms are the unifying characteristic within the phonetic class of laterals and within the phonetic class of rhotics; constriction location serves to differentiate members within each class.

In Tamil phonology, the laterals pattern differently from the rhotics. With respect to their phonotactic distribution, the laterals are systematically more consonant-like. For example, the laterals along with nasal, stop, and fricative consonants occur singly or as geminates; whereas the rhotics, like the glides, occur only singly. Furthermore, rhotics and glides can occur before a tautosyllabic consonant. Laterals and all other consonants are banned from this position. The rhotics, like vowels, lack medial tongue-palate closure (or near closure as seen in fricatives) and instantiate simple articulatory-acoustic relations that are predictable, a characteristic associated with vowels more than with consonants.

1. Descriptive classification

Let us begin with the class of laterals. The mechanisms of [ɭ] production are the same as those of [l]: an oral constriction along the midsagittal line is formed, lateral channels along the sides of the tongue are created, and a convex posterior tongue body surface facilitates coupling between the front and back cavities. In addition, [ɭ] and [l] share similarly shaped (i.e., skewed) velocity profiles (intermediate values of proportional time to peak velocity). It is proposed that these mechanisms characterize the class Lateral. The Tamil laterals are distinguished from each other by means of the location of the tongue blade constriction: the medial oral constriction for [ɭ] occurs in the palatal region, while the constriction for [l] is alveolar. In terms of dynamics, the constriction formation and release durations, pathlengths, and velocities of [ɭ] are greater than those of [l]. The retroflex lateral [ɭ] has a larger front cavity and a correspondingly low front-cavity resonance value ($F3$), thus distinguishing it acoustically from [l].

The similarity in tongue shaping for the rhotic class is even more striking. In particular, it was seen above that tongue shaping is essentially identical for [r] and [r̲]: a raised tongue-tip (apical) constriction, a tongue body gradually lowered in the antero-posterior direction, and slight concavity of the tongue surface. Additionally, [r] and [r̲] share similarly shaped (i.e., skewed) velocity profiles (late proportional time-to-peak velocity). The members of this category are distinguished from one another by constriction location, [r] being articulated with a slightly more anterior tongue constriction than [r̲]. In terms of contrast in dynamics, [r̲] has greater constriction pathlengths and velocity values than [r], but somewhat overlapping duration values.

The articulatory data justify the postulation of a class of rhotics and a class of laterals in Tamil, but do not provide evidence in favor of a larger class of liquids. Such a superclass appears to have largely an acoustic basis. Both rhotics and laterals are voiced sonorants and have similarities in formant structure. The first formant (400–500 Hz) is due to the Helmholtz resonance of back-cavity constriction. The second formant (1200–1600 Hz) is the lowest resonance of the back cavity. (Note that, as discussed in Sec. III, the value of the third formant, which distinguishes members of the liquid class from one another—around 2400 Hz for [l] and significantly less for the other liquids—is influenced by where and how the oral constriction is formed.) In the liquid class the first three formants are most prominent, while higher formants are strongly reduced in intensity, typically due to zeroes in the spectra. The articulatory origin of the zeroes varies: they may arise due to sublingual space, as in the case of certain rhotics, or due to side-channel effects, as in case of laterals. However, the presence of a zero in the region of high formants, along with voicing and a common $F1$ and $F2$ structure, is another acoustic characteristic of the class of liquids.

Let us next turn to the more elusive consonant /ɽ/. Based on the theory outlined above, we are now in a position to place /ɽ/ within one of the segment classes of Tamil in a principled manner. The overall tongue shape mechanisms of /ɽ/ clearly are not those associated with the production of the lateral class. The laterals are characterized by medial tongue closure, a laterally inward drawn tongue body, and a convex posterior tongue surface. The segment /ɽ/ involves no medial closure, a lateral bracing of the tongue body, and a concave posterior tongue surface. The rhotics /r/ and /r̲/ have in common with /ɽ/ a medial tongue-tip constriction (but no closure) and an absence of lateral channels. Furthermore, the tongue surface contour behind the oral constriction is concave in /r/ and /r̲/, and even more so in /ɽ/. From this it can be concluded that the Tamil /ɻ/ is properly categorized as a rhotic.

Our data have provided us with hitherto unavailable information regarding the production of Tamil liquids. This information has allowed us to propose a principled system of liquid categorization and demonstrates that the classification of /ɻ/ as anything other than a rhotic is without justification.

Two questions may be posed now. First, why has /ɻ/ often been categorized as a lateral? And, second, what articulatory-acoustic relations play a role in dialectal substitutions and mergers that occur among these liquids? The latter question is addressed in the following section. In regards to the first question, it is our view that the affinity between /ɭ/ and /ɻ/ is based on their extreme retroflexion. This retroflexion gives rise to a large front cavity and, consequently, an acoustic similarity between /ɭ/ and /ɻ/. In particular, both exhibit proximity of $F2$ and $F3$. There is a dynamic affinity between /ɭ/ and /ɻ/ as well. While in /r/ and /r̲/, tongue-tip peak velocity is attained proportionally late, in /ɻ/ and the laterals (particularly /ɭ/), peak velocity is reached proportionally early. Also, due to their retroflex articulation, the tongue-tip constriction formation and release curvature is counterclockwise (i.e., back-to-front) in both /ɭ/ and /ɻ/. It is thus understandable and correct that /ɭ/ and /ɻ/ should be grouped together in classification—both are retroflex sounds.

2. Linguistic substitutions and mergers

Recall that dialectal substitutions and mergers are known to take place among these liquids. In some dialects the acoustically similar /r/ and /r̲/ have merged or are in the process of merging (Christdas, 1988, p. 131). It was shown that for this speaker these sounds are produced with a tongue-tip constriction that differs only minimally in horizontal position (see Fig. 5), and that these sounds share a similar formant structure. Overall for this speaker the distinction between /r/ and /r̲/ is fragile in both the articulatory and auditory domains. Small variations in the production of either or both sounds would be likely to obliterate this subtle distinction. Thus we speculate that the linguistic merger of Tamil /r/ and /r̲/ might be a consequence of minimal articulatory distinction and substantial auditory overlap.

Furthermore, certain Tamil speakers exhibit substitution of /ɭ/ for /ɻ/ (Christdas, 1988, p. 160). Recall that for the speaker in the present study, /ɭ/ and /ɻ/ share similar acoustic spectral characteristics, particularly in their first three formants. In particular, both /ɭ/ and /ɻ/ have a low $F3$ frequency close to that of $F2$, due to a relatively long front cavity. Recall also from the MRI and palatography data that the production of /ɻ/ involves, in addition to creating the retroflex constriction, a pitted posterior tongue cavity. The posterior tongue body shaping for /ɻ/ involves coordination of both internal tongue muscles and external forces provided by linguapalatal bracing. For /ɭ/, on the other hand, the posterior tongue body shaping is primarily executed by internal muscular action. Further, both the absolute time-to-peak velocity *and* the proportional time-to-peak velocity of the tongue tip are earlier in /ɻ/ than /ɭ/. The remaining liquids, /r/ and /r̲/, which have the latest proportional time-to-peak velocity of the tongue tip, are characterized by the simplest tongue shapes. This is consistent with the notion that tip peak velocity is reached comparatively earlier in sounds that require more complex tongue body shaping. We speculate that it is perhaps the more complex tongue-shaping requirement, above and beyond the creation of a retroflex constriction, for producing /ɻ/ that is compromised in the neutralization of the /ɭ/–/ɻ/ contrast by some speakers yielding the single variant /ɭ/.

3. Dimensions of contrast

The diversity of tongue shapes and dynamics are made possible, at least in part, through different lingua-palatal bracing mechanisms (see Stone *et al.*, 1991, 1992; Narayanan *et al.*, 1997; Alwan *et al.*, 1997). The tongue shape geometry and the temporal characteristics of their realization give rise to systematic differences in the acoustic resonance behavior of the vocal tract. These data suggest that speech production targets go beyond simple constriction targets in the midsagittal plane. This is not surprising considering the complexity of behavior possible for the tongue, ''a boneless, jointless structure...[that] can elevate, depress, widen, narrow, extend, and retract...and move differentially, both laterally-to-medially and left-to-right'' (Stone *et al.*, 1991). The targets that the speech production system works to attain by calling on these many degrees of freedom must be able to yield complex tongue shapes, such as the pitted tongue surface contour observed for [ɻ] articulation. Furthermore, our data also suggest that different aspects of vocal tract configuration (e.g., tongue position and shape) are constrained in a phoneme-specific manner. For example, among the five liquids, [ɻ] exhibits the most variability in tongue-tip position while being fairly consistent in tongue shaping. When compared to the laterals this is understandable because the tongue tip is free in [ɻ] and not in the laterals. Rhotics [r] and [r̲] could in principle exhibit variability, but in fact, only [ɻ] shows significant tongue-tip position variability. The two anterior rhotics are only subtly distinct; any divergence from prototypical tongue-tip position would be likely to increase the chance of confusion between the two phones. (In those dialects exhibiting [r]–[r̲] merger, one might speculate that tongue-tip freedom has given rise to acoustic overlap.) In summary, this suggests that for certain sounds the realization of a particular constriction position may be less narrowly constrained than is the realization of tongue shape for that sound.

B. Comparison to English liquids

The liquids of Tamil and English can be compared using published articulatory and acoustic data on English liquids. Articulatory data on English /l/'s have been obtained using various techniques such as x-ray imaging (Giles and Moll, 1975), magnetometry (Sproat and Fujimura, 1993), ultrasound imaging (Stone *et al.*, 1992), MRI (Narayanan *et al.*, 1997), and electropalatography (Stone *et al.*, 1992; Narayanan *et al.*, 1997). Espy-Wilson (1992) provides a comprehensive characterization of the acoustics of American English /l/. In English, the lateral approximant is voiced and has been broadly classified into light and dark varieties, occurring typically in pre-vocalic and post-vocalic contexts, respectively. Both types, in general, show contact of the anterior tongue in the dental or alveolar region and an inward lateral compression of the posterior tongue body (toward the midsagittal plane) that facilitates the creation of lateral channels along the sides of the tongue. The areas of these channels are typically unequal. The contours of the tongue surface cross-sections are convex.

The articulatory and acoustic characteristics of the Tamil dental [l] and the American English (AE) [l] appear very similar. Both have tongue-tip constrictions in the dental region, lateral linguapalatal contacts of the anterior tongue, convex tongue surface contours, and side airflow channels created by a laterally inward-drawn tongue body. Like the AE [l], the dental [l] in Tamil can appear in both syllable-initial and -final positions, word-initially, and word-finally. The dark AE [l], usually appearing syllable-finally, is typically characterized by narrow upper pharyngeal areas due to high position of the posterior tongue body raising and retraction of the tongue root (Sproat and Fujimura, 1993; Narayanan *et al.*, 1997). Such ''pharyngealization'' contributes to $F2$ lowering in dark [l] when compared to light [l]. The MRI data of the Tamil [l] also shows such pharyngealization. Recall that the Tamil [l] was produced in the /paC/ context during the MRI experiment. Unfortunately, it is not possible to tell from the MRI data whether there are any systematic differences in the phonetic implementation of [l] depending on its relative position within the syllable. (The magnetometer procedure in turn offers no information on tongue root position.)

The production of English /ɹ/ has been observed to exhibit considerable variability in its articulatory configurations (Delattre and Freeman, 1968; Alwan *et al.*, 1997; Westbury *et al.*, 1998). Nonetheless, /ɹ/ shows acoustic stability, i.e., different vocal tract shapes yield essentially equivalent acoustic output. English /ɹ/ is characterized by a stable acoustic pattern of lowering of the third formant frequency close to that of the second formant (Boyce and Espy-Wilson, 1997). It has long been claimed, for instance, that American English /ɹ/ can be either ''retroflex'' or ''bunched'' (Ladefoged and Maddieson, 1996). In fact, the /ɹ/ of English exhibits a continuum of vocal tract shapes across speakers that yields a regular acoustic output (Delattre and Freeman, 1968; Lindau, 1985; Alwan *et al.*, 1997; Boyce and Espy-Wilson, 1997; Westbury *et al.*, 1998; see also Guenther *et al.*, 1999).

The pre- and post-alveolar /r/'s of Tamil do not show much variation in their vocal tract configurations. (As linguistically contrasting, it is not a surprise that the articulations of these sounds are largely kept distinct.) Interestingly, these sounds occupy adjacent and somewhat overlapping regions of the articulatory continuum identified for English. The relevant region is that which characterizes the so-called ''tip-up'' American English /ɹ/ (cf. Delattre and Freeman's British ''retroflex'' /ɹ/). Given that the tongue shape continuum for English corresponds to a unified acoustic outcome, and given that the Tamil /r/ and /r̠/ fall on this continuum, these Tamil sounds are expected to share a similar formant structure. This expectation is borne out.

American English lacks strongly retroflexed sounds, nonetheless a fruitful comparison between English /ɹ/ and Tamil /ɻ/ can be made. Such a comparison serves to demystify the elusive /ɻ/. The Tamil /ɻ/ shares important properties with the English rhotic—particularly the ''bunched'' variety—although it does not fall directly on the same vocal tract shape continuum. In both sounds, the raised anterior tongue (bunched in AE /ɹ/, retroflexed in Tamil /ɻ/) is accompanied by a prominently concave posterior tongue region that appears as a pitted cavity. In both AE (Alwan *et al.*, 1997) and Tamil, the posterior tongue body shaping is facilitated by bracing of the tongue body against the palate. The dimensions of this pitted back cavity are similar in both sounds and yield similar Helmholtz resonances ($F1$). Low $F3$ values in both languages result from a relatively large front cavity. Both languages achieve this by means of an inward-drawn anterior tongue (for AE Alwan *et al.*, 1997), although the front-cavity volume for Tamil /ɻ/ is slightly larger because the tongue tip, rather than the tongue body, is retracted. Thus while both the AE /ɹ/ and Tamil /ɻ/ are rather exotic sounds cross-linguistically, they turn out to be surprisingly similar both articulatorily and acoustically.

V. CONCLUDING REMARKS

The articulatory characterization of Tamil's unusual set of five contrasting liquids has been examined both in terms of articulatory geometry and kinematics. Although the study depended on only a single experimental subject, the use of multiple techniques for investigating both static and dynamic articulatory characteristics—static palatography, magnetic resonance imaging (MRI), and magnetometry (EMMA)—has helped provide a better understanding of the production dynamics and articulatory-acoustic mappings for these liquids.

Current models of speech production often assume that constriction position, defined in the midsagittal plane, is the main ''place of articulation'' parameter. However, this study suggests that articulation cannot be characterized solely by identifying constriction position. Rather, three-dimensional tongue shape and the dynamics underlying shape formation are critical to understanding natural linguistic classes and phonological phenomena.

ACKNOWLEDGMENTS

Work supported in part by NSF Grant No. IRI-9503089 (S.N.) and NIH Grants Nos. DC-03172, DC-00016 (D.B., Haskins Laboratories). The authors wish to acknowledge the technical support of Kate Haker (Cedars-Sinai Hospital, Los Angeles, CA), and Louis Goldstein and Walter Naito (Haskins Laboratories, New Haven, CT). The authors thank Abeer Alwan and Peter Ladefoged for their expertise and advice; and Pierre Badin, Carol Espy-Wilson, and an anonymous reviewer for their helpful comments.

APPENDIX A: STIMULI AS PRESENTED TO THE SUBJECT FOR THE EMMA EXPERIMENT. AN ENGLISH GLOSS HAS BEEN ADDED TO RIGHT

Andha vakyam ‘‘kali’’ perusu.	The utterance ‘‘fate’’ is-big.
Andha vakyam ‘‘kaLi’’ perusu.	...‘‘pudding’’...
Andha vakyam ‘‘kazhi’’ perusu.	...‘‘pole’’...
Andha vakyam ‘‘kari’’ perusu.	...‘‘coal’’...
Andha vakyam ‘‘kaRi’’ perusu.	...‘‘curry’’...
Andha vakyam ‘‘pali’’ perusu.	...‘‘sacrifice’’...
Andha vakyam ‘‘paLi’’ perusu.	...nonce...
Andha vakyam ‘‘pazhi’’ perusu.	...‘‘blame’’...
Andha vakyam ‘‘pari’’ perusu.	...‘‘horse’’...
Andha vakyam ‘‘paRi’’ perusu.	...‘‘pluck’’...
Andha vakyam ‘‘val’’ perusu.	...‘‘tail’’...
Andha vakyam ‘‘vaL’’ perusu.	...‘‘sword’’...
Andha vakyam ‘‘vazh’’ perusu.	...‘‘live’’...
Andha vakyam ‘‘var’’ perusu.	...‘‘strap’’...
Andha vakyam ‘‘vaR(pu)’’ perusu.	...‘‘mold’’...
Andha vakyam ‘‘alai’’ perusu.	...‘‘wave’’...
Andha vakyam ‘‘aLai’’ perusu.	...‘‘sift’’...
Andha vakyam ‘‘azhai’’ perusu.	...‘‘invite’’...
Andha vakyam ‘‘arai’’ perusu.	...‘‘half’’...
Andha vakyam ‘‘aRai’’ perusu.	...‘‘room’’...
Andha vakyam ‘‘palam’’ perusu.	...‘‘strength’’...
Andha vakyam ‘‘paLam’’ perusu.	...nonce...
Andha vakyam ‘‘pazham’’ perusu.	...‘‘fruit’’...
Andha vakyam ‘‘param’’ perusu.	...‘‘almighty’’...
Andha vakyam ‘‘paRam’’ perusu.	...nonce...
Andha vakyam ‘‘vaLi’’ perusu.	...‘‘wind’’...
Andha vakyam ‘‘vaLam’’ perusu.	...‘‘fertile’’...
Andha vakyam ‘‘paRavai’’ perusu.	...‘‘bird’’...

APPENDIX B: AREA FUNCTIONS FROM MRI DATA FOR THE FIVE TAMIL LIQUIDS

A graphical representation is provided in Fig. 9.

D_{lips}[a] (cm)	Cross-sectional areas (mm^2)				
	[l]	[ɭ]	[r]	[r̠]	[ɽ]
0.43	267.63	375.29	299	300	418.8
0.86	351.78	391.99	264.11	264.33	309.16
1.29	254.44	487.79	358.59	239.94	312.23
1.72	0	406.71	20.27	340.14	271.36
2.15	0	434.18	74.27	20.25	342.55
2.58	68.45	595.02	93.1	86.46	480.32
3.01	101.23	637.43	171.61	126.86	639.62
3.44	182.81	687.08	289.6	231.81	750.17
3.87	296.63	335.23	392.43	346.07	455.05
4.30	417.7	89.87	343.65	375.07	223.87
4.73	407.15	0	412.21	390.01	17.23
5.16	361.01	0	341.89	414.38	19.95
5.59	350.9	166	320.14	434.72	173
6.02	291.8	299.21	215.99	415.94	311.8
6.45	252.91	310.91	177.1	382.1	396.3
6.88	243.92	373.97	154.69	330.25	412.21
7.31	252.47	367.16	128.1	319.04	421.44
7.74	250.49	418.8	135.13	296.19	440
8.17	148.97	372.22	134.69	221.7	489.12
8.6	120.85	191.6	121.95	136.89	399.68
9.03	101.95	258.4	116.24	96.9	283.45
9.46	128.76	300.37	106.79	68.55	316.41
9.89	90.75	273.56	90.97	54.49	340.14
10.32	57.57	254.25	86.57	59.77	260.74
10.75	41.53	198.85	83.06	74.71	232.47
11.18	58.67	160.62	108.11	88.11	210.94
11.61	61.52	144.14	108.54	82.84	228.52
12.04	76.46	156.67	167.43	124.37	196.44
12.47	97.12	161.23	112.72	151.22	186.11
12.9	165.89	172.49	144.58	183.03	220
13.33	225.43	224.34	222.8	172.49	249.39
13.76	327.54	264.99	281.03	242.58	329.59
14.19	303	315.75	352	251.59	371.78
14.62	193.8	310.63	349.58	128.1	373.97
15.05	108.98	57.55	77.12	43.73	218.63
15.48	72.73	55.81	64.16	39.11	53.83
15.91	36.47	59.33	68.33	40.43	40
16.34	55.37	102.83	124.58	72.29	94.48
16.77	111.4	78.66	108.98	73.61	167.87
17.2	141.94	164.36	217.53	205.44	174.02

[a]D_{lips} (in cm) is distance from the lip opening.

D_{lips}[a] (cm)	Sublingual areas (mm^2) [r]	D_{lips}[a] (cm)	Sublingual areas (mm^2) [r̠]
1.72	258.40	2.15	269.58
2.15	181.39	2.58	166.11
2.58	164.79	3.01	119.97
3.01	75.81	3.44	107.23
3.44	33.18	3.87	22.63

[a]D_{lips} (in cm) is distance from the lip opening.

D_{lips}[a] (cm)	Lateral channel areas (mm^2) [l]	D_{lips}[a] (cm)	Lateral channel areas (mm^2) [ɭ]
1.72	47.90	4.73	34.94
2.15	64.60	5.16	59.21
2.58	161.94	5.59	90.70
3.01	156.88	6.02	118.43
3.44	162.38	6.45	103.24
3.87	113.15	6.88	77.13
4.30	92.72	7.31	67.24
4.73	68.33	7.74	44.38

[a]D_{lips} (in cm) is distance from the lip opening.

[1]Note that this means that no tokens of word final retroflex [ɭ] could be included in the analysis. Such multiple velocity extrema are typical of slowed speech. Why this particular liquid should be especially subject to this effect is an open question.

[2]The fact that their *y*-values are the same does not mean that they are effectively equivalent. Due to the rising slope of the alveolar ridge, [l] achieves complete closure while [r̠], with the same *y*-value, achieves only approximation.

[3]Recall also that 17 word final tokens were excluded due to multiple tangential velocity minima at the peak. This velocity profile pattern is characteristic of slowed articulations. Thus, it seems likely that the 17 excluded tokens also underwent considerable word-final lengthening.

Alwan, A., Narayanan, S., and Haker, K. (**1997**). ‘‘Toward articulatory-acoustic models for liquid approximants based on MRI and EPG data. Part

II. The rhotics,'' J. Acoust. Soc. Am. **101**, 1078–1089.
Balasubramanian, T. (**1972**). ''The phonetics of colloquial Tamil,'' Ph.D. dissertation, University of Edinburgh, Edinburgh.
Boyce, S., and Espy-Wilson, C. (**1997**). ''Coarticulatory stability in American English /r/,'' J. Acoust. Soc. Am. **101**, 3741–3753.
Byrd, D., and Saltzman, E. (**1998**). ''Intragestural dynamics of multiple phrasal boundaries,'' J. Phonetics **26**, 173–199.
Christdas, P. (**1988**). ''The phonology and morphology of Tamil,'' Ph.D. dissertation, Cornell University, Ithaca, NY.
Delattre, P., and Freeman, D. C. (**1968**). ''A dialect study of American r's by x-ray motion picture,'' Linguistics, An international review **44**, 29–68.
Espy-Wilson, C. (**1992**). ''Acoustic measures for linguistic features distinguishing the semivowels in American English,'' J. Acoust. Soc. Am. **92**, 736–757.
Espy-Wilson, C., Narayanan, S., Boyce, S., and Alwan, A. (**1997**). ''Acoustic modelling of American English /r/,'' Proceedings of Eurospeech 97, Rhodes, Greece, pp. 393–396.
Fant, G. (**1968**). ''Analysis and synthesis of speech processes,'' in *Manual of Phonetics*, edited by B. Malmberg (North-Holland, Amsterdam), pp. 171–272.
Flanagan, J. (**1972**). *Speech Analysis, Synthesis and Perception* (Springer-Verlag, New York).
Giles, S. B., and Moll, K. L. (**1975**). ''Cineflurographic study of selected allophones of English [l],'' Phonetica **31**, 206–227.
Gracco, V. L., and Nye, P. W. (**1993**). ''Magnetometry in speech articulation research: Some misadventures on the road to enlightenment,'' Forschungsberichte des Institut für Phonetic und Sprachliche Kommunikation der Universität München (FIPKM) **31**, 91–104.
Guenther, F. H., Espy-Wilson, C., Boyce, S., Matthies, M., Zandipour, M., and Perkell, J. (**1999**). ''Articulatory tradeoffs reduce acoustic variability during American English /r/ production,'' J. Acoust. Soc. Am. **105**, 2854–2865.
Kelso, J. A. S., Vatikiotis-Bateson, E., Saltzman, E. L., and Kay, B. (**1985**). ''A qualitative dynamic analysis of reiterant speech production: Phase portraits, kinematics, and dynamic modeling,'' J. Acoust. Soc. Am. **77**, 266–280.
Ladefoged, P. (**1957**). ''Use of palatography.'' Journal of Speech and Hearing Disorders **22**, 764–774.
Ladefoged, P. (**1982**). *A Course in Phonetics* (Harcourt Brace Jovanovich, New York).
Ladefoged, P., and Maddieson, I. (**1996**). *The Sounds of the World's Languages* (Blackwell Publishers, Cambridge, MA).
Lindau, M. (**1985**). ''The story of r,'' in *Phonetic Linguistics*, edited by V. Fromkin (Academic, Orlando, FL), pp. 157–168.
Löfqvist, A. (**1993**). ''Electromagnetic transduction techniques in the study of speech motor control,'' Reports from the Department of Phonetics, University Umeå, PHONUM **2**, 87–106.
Löfqvist, A., Gracco, V., and Nye, P. (**1993**). ''Recording speech movements using magnetometry: One laboratory's experience,'' Forschungsberichte des Institut für Phonetic und Sprachliche Kommunikation der Universität München (FIPKM), **31**, 143–162.
Narayanan, S., Alwan, A., and Haker, K. (**1995**). ''An articulatory study of fricative consonants using magnetic resonance imaging,'' J. Acoust. Soc. Am. **98**, 1325–1347.
Narayanan, S., Alwan, A., and Haker, K. (**1997**). ''Toward articulatory-acoustic models for liquid approximants based on MRI and EPG data. Part I. The laterals,'' J. Acoust. Soc. Am. **101**, 1064–1077.
Narayanan, S., and Alwan, A. (**1996**). ''Parametric hybrid source models for voiced and voiceless fricative consonants,'' Proceedings of ICASSP **96**, pp. 337–340.
Narayanan, S., Kaun, A., Byrd, D., Ladefoged, P., and Alwan, A. (**1996**). ''Liquids in Tamil,'' edited by H. T. Bunnell and W. Idsardi, Proceedings of ICSLP 96, pp. 797–800.
Narayanan, S., and Kaun, A. (**1999**). ''Acoustic modeling of retroflex Tamil liquids,'' Proceedings of XIV ICPhS, San Francisco, CA (in press).
Ostry, D. J., and Munhall, K. (**1985**). ''Control of rate and duration of speech movements,'' J. Acoust. Soc. Am. **77**, 640–648.
Perkell, J., Cohen, M., Svirsky, M., Matthies, M., Garabieta, I., and Jackson, M. (**1992**). ''Electro-magnetic midsagittal articulometer (EMMA) systems for transducing speech articulatory movements,'' J. Acoust. Soc. Am. **92**, 3078–3096.
Ramasubramanian, N., and Thosar, R. (**1971**). ''Synthesis by rule of some retroflex speech sounds,'' Language and Speech **14**, 65–85.
Rubin, P. E. (**1995**). ''HADES: A case study of the development of a signal analysis system,'' in *Applied Speech Technology* (CRC Press, Boca Raton, FL), pp. 501–520.
Saltzman, E., Löfqvist, A., and Mitra, S. (**in press**). '' 'Clocks' and 'glue'—Global timing and intergestural cohesion,'' Papers in Laboratory Phonology V.
Scheffé, H. (**1953**). ''A method for judging all contrasts in the analysis of variance,'' Biometrika **40**, 87–104.
Sproat, R., and Fujimura, O. (**1993**). ''Allophonic variation in English /l/ and its implications for phonetic implementation.'' J. Phonetics **21**, 291–311.
Stevens, K. (**1998**). *Acoustic Phonetics* (MIT Press, Cambridge, MA).
Stone, M., Faber, A., Cordaro, M. (**1991**). ''Cross-sectional tongue movement and tongue-palate movement in [s] and [ʃ] syllables,'' Proceedings of the XII ICPhS, pp. 354–357.
Stone, M., Faber, A., Raphael, L., and Shawker, T. (**1992**). ''Cross-sectional tongue shapes and linguopalatal contact patterns in [s], [S] and [l] syllables.'' J. Phonetics **20**, 253–270.
Westbury, J. R., Hashi, M., and Lindstrom, M. J. (**1998**). ''Differences among speakers in lingual articulations for American English /''trnr''/,'' Speech Commun. **26**, 203–226.